



HAL
open science

”Classical” Electroporabilization Modeling at the Cell Scale

Otared Kavian, Michael Leguèbe, Clair Poignard, Lisl Weynans

► **To cite this version:**

Otared Kavian, Michael Leguèbe, Clair Poignard, Lisl Weynans. ”Classical” Electroporabilization Modeling at the Cell Scale. [Research Report] RR-8005, 2012. hal-00712683v1

HAL Id: hal-00712683

<https://inria.hal.science/hal-00712683v1>

Submitted on 27 Jun 2012 (v1), last revised 5 Dec 2012 (v3)

HAL is a multi-disciplinary open access archive for the deposit and dissemination of scientific research documents, whether they are published or not. The documents may come from teaching and research institutions in France or abroad, or from public or private research centers.

L’archive ouverte pluridisciplinaire **HAL**, est destinée au dépôt et à la diffusion de documents scientifiques de niveau recherche, publiés ou non, émanant des établissements d’enseignement et de recherche français ou étrangers, des laboratoires publics ou privés.



“Classical” Electropermeabilization Modeling at the Cell Scale

O. Kavian¹, M. Leguèbe², C. Poignard², L. Weynans²

¹ Département de Mathématiques, LMV CNRS UMR8100,
Université Versailles-Saint-Quentin-en-Yvelines, France

² Team MC2, INRIA Bordeaux-Sud-Ouest & CNRS UMR 5251,
Université de Bordeaux, France

**RESEARCH
REPORT**

N° 8005

June 2012

Project-Teams MC2



“Classical” Electroporation Modeling at the Cell Scale

O. Kavian¹, M. Leguèbe², C. Poignard^{2*}, L. Weynans²

¹ Département de Mathématiques, LMV CNRS UMR8100,
Université Versailles-Saint-Quentin-en-Yvelines, France

²Team MC2, INRIA Bordeaux-Sud-Ouest & CNRS UMR 5251,
Université de Bordeaux, France

Project-Teams MC2

Research Report n° 8005 — June 2012 — 27 pages

Abstract: In this paper we derive two models (a static and a dynamical model) based on the description of the electric potential in a biological cell in order to model the cell electroporation. Existence and uniqueness results for each model are provided, and accurate numerical method to compute the solution is presented. We then present numerical results that corroborate the experimental results, justifying the validity of our modeling. We emphasize that our new models involve very few parameters, compared with the most achieved model but they describe the same qualitative results. Moreover our numerical results are quantitatively close to the experimental data.

Key-words: Cell modeling, non-linear partial differential equations, Finite differences on cartesian grids

* Corresponding author: clair.poignard@inria.fr

**RESEARCH CENTRE
BORDEAUX – SUD-OUEST**

351, Cours de la Libération
Bâtiment A 29
33405 Talence Cedex

“Classical” Electroporabilization Modeling at the Cell Scale

Résumé : In this paper we derive two models (a static and a dynamical model) based on the description of the electric potential in a biological cell in order to model the cell electroporabilization. Existence and uniqueness results for each model are provided, and accurate numerical method to compute the solution is presented. We then present numerical results that corroborate the experimental results, justifying the validity of our modeling. We emphasize that our new models involve very few parameters, compared with the most achieved model but they describe the same qualitative results. Moreover our numerical results are quantitatively close to the experimental data.

Mots-clés : Cell modeling, non-linear partial differential equations, Finite differences on cartesian grids

Contents

1	Introduction	4
1.1	Electric potential in a biological cell	4
1.2	Electropermeabilization phenomenon	5
1.3	Modeling principle	5
2	The static equation	6
2.1	Existence and uniqueness of the static potential	7
3	The dynamical model	10
3.1	Heuristics of the modeling	10
3.2	Statement of the mathematical problem	12
3.3	Resolution of the differential equation (24)	12
3.4	Existence and uniqueness	14
4	Numerical simulations	17
4.1	Spatial discretization	17
4.2	Accuracy of the method	18
4.3	Computation of the non-linear static model	19
4.3.1	Influence of the parameter S_{ir}	20
4.3.2	Comparison with the model of Ivorra <i>et al.</i>	20
4.4	The dynamical problem	20
4.4.1	Time-discretization method of the model	20
4.4.2	Main parameters influence	22
4.4.3	Comparison with Neu and Krassowka models	22
4.4.4	Static vs dynamical model	25
5	Conclusion	25

1 Introduction

The distribution of the electric potential in a biological cell is important for bio-electromagnetic investigations. A sufficiently large amplitude of the transmembranar potential (TMP), which is the difference of the electric potentials between both sides of the cell membrane, leads to an increase of the membrane permeability [19, 23]. Molecules such as bleomycin can then diffuse across the plasma membrane. This phenomenon, called electropermeabilization, has already been used in oncology and holds promises in gene therapy [11, 20], justifying precise assessments of the TMP.

In this paper we aim at studying theoretically and numerically a non-linear electrical model of biological cells. This model is inspired from the static model of Ivorra *et al.* in [10]. It describes the behaviour of both electric potential and membrane conductivity when the cell is submitted to an electric pulse through few parameters that will be fitted with the experiments. We emphasize that this is a phenomenological model in the sense that the membrane conductivity is described by an *ad hoc* law and does not come from an homogenization of the nanoscale phenomena. Before stating the model we are going to study let us present the notations.

Notation 1.1. *Throughout this paper we shall use the following conventions and notations:*

- We generically denote by \mathbf{n} the normal to a closed smooth surface of \mathbb{R}^3 (or a curve of \mathbb{R}^2) outwardly directed to the domain enclosed by the surface or the curve.
- Let \mathcal{C} be a surface of \mathbb{R}^3 , and let u be a sufficiently smooth function (in an appropriate sense) defined in a tubular neighbourhood of \mathcal{C} . We define $u|_{\mathcal{C}^\pm}$ by

$$\forall x \in \mathcal{C}, \quad u|_{\mathcal{C}^\pm}(x) = \lim_{\tau \rightarrow 0^+} u(x \pm \tau \mathbf{n}(x)),$$

and $\partial_{\mathbf{n}}u|_{\mathcal{C}^\pm}$ and $\partial_{\mathbf{t}}u|_{\mathcal{C}^\pm}$ will denote the normal and the tangential components of ∇u ,

$$\begin{aligned} \forall x \in \mathcal{C}, \quad \partial_{\mathbf{n}}u|_{\mathcal{C}^\pm}(x) &= \lim_{\tau \rightarrow 0^+} \nabla u(x \pm \tau \mathbf{n}(x)) \cdot \mathbf{n}(x), \\ \partial_{\mathbf{t}}u|_{\mathcal{C}^\pm}(x) &= \nabla u(x) - \partial_{\mathbf{n}}u(x)\mathbf{n}(x), \end{aligned}$$

where the dot “ \cdot ” denotes the Euclidean scalar product of \mathbb{R}^3 . In the case of \mathbb{R}^2 the analogous notations are easily adapted.

- The jump $[u]_{\mathcal{C}}$ of a function u defined in a neighbourhood of the surface \mathcal{C} is defined by

$$[u]_{\mathcal{C}} = u|_{\mathcal{C}^+} - u|_{\mathcal{C}^-}.$$

- Observe that for a sufficiently smooth function v defined in a neighborhood of Γ , we have:

$$\mathbf{n}_i \cdot \nabla v|_{\Gamma^-} = \partial_{\mathbf{n}}u|_{\Gamma^-}, \quad \text{and} \quad \mathbf{n}_e \cdot \nabla v|_{\Gamma^+} = -\partial_{\mathbf{n}}u|_{\Gamma^+}.$$

1.1 Electric potential in a biological cell

A biological cell is a high contrast medium composed of a conducting cytoplasm \mathcal{O}_c surrounded by a thin and very insulating layer. The plasma membrane is a phospholipid bilayer sprinkled over with a few proteins. Due to its thickness and its electrical properties the membrane can be modeled as a surface electric material Γ with a capacity C_m and a surface conductivity S_m . We refer to the seminal works of Hodgkin, Goldman, Katz *et al.* for the electric description of cell membranes [5, 7, 9, 8]. As described by Neu, Krassowska and DeBruin [14, 3] the electric

potential in the whole cell embedded in a bath \mathcal{O}_e is the discontinuous solution U of the following problem

$$\Delta U = 0, \quad \text{in } \mathcal{O}_e \cup \mathcal{O}_c, \quad (1a)$$

$$U(0, \cdot) = 0, \quad \text{and for all } t > 0, \quad (1b)$$

$$U(t, x) = g(t, x), \quad \text{on } \partial\Omega \quad (1c)$$

with the transmission conditions across the membrane Γ :

$$[\sigma \partial_{\mathbf{n}} U]_{\Gamma} = 0, \quad (1d)$$

$$C_m \partial_t [U]_{\Gamma} + S_m [U]_{\Gamma} = \sigma_c \partial_{\mathbf{n}} U|_{\Gamma^-}. \quad (1e)$$

1.2 Electroporpermeabilization phenomenon

When submitted to a high electric pulse — *i.e.* if the amplitude of the pulse g reaches a threshold value — the cell membrane permeability increases and large molecules that usually cannot diffuse through the plasma membrane (for instance, plasmids or bleomycin) enter inside the cytoplasm. This phenomenon is called *electroporation* or *electroporpermeabilization*. For several years different membrane models based on hydrodynamic, elasticity, hydroelasticity, viscoelasticity or aqueous pore formation have been developed to describe the pore formation on the cell membrane (for more details, see the review of Pavlin *et al.* [17]). They all highlight a threshold value of the electric potential above which the electroporpermeabilization phenomenon occurs. However, the critical potential value changes with the models. Theoretical biophysicists consider the aqueous pore formation model as the most convincing current explanation. Nevertheless the model predictions do not coincide with experiments, either quantitatively or phenomenologically. In addition, the models essentially based on the paper of Neu, Krassowska *et al.* [14, 3, 4] are too complex to be parameterized to fit the experiments. Roughly speaking, the current models provide a qualitative explanation of the electroporpermeabilization, but the problem of the quantitative description remains open.

Actually *in vitro* and *in vivo* experiments have never proved the electropore formation, which theoretically could reach detectable size (since macropores could be created according to Smith *et al.* [21]) and it seems unclear that whether electroporation results from holes punched in a lipid bilayer as proposed in the current models (Teissié *et al.* [23, 22]). Moreover the experimentally proved reversible process of the membrane electroporation is not clearly explained by the current models. In addition, and this is probably one of the main features of the experiments that is not yet explained, at the level of the changes in structure of the electroporpermeabilized membranes the *vectorization* of large molecules requires both short time high-voltage pulses and long time low-voltage pulses (André *et al.* [1]). For all these reasons we prefer the term *electroporpermeabilization* to *electroporation*.

1.3 Modeling principle

The probably most achieved electroporpermeabilization model has been obtained by Neu and Krassowska [14] and precisely described by DeBruin and Krassowska [3, 4]. It consists in adding an electroporation current I_{ep} in the right-hand side of equation (1e):

$$C_m \partial_t [U]_{\Gamma} + S_m [U]_{\Gamma} = \sigma_c \partial_{\mathbf{n}} U|_{\Gamma^-} + I_{ep}.$$

The current I_{ep} is given by a highly non-linear pore current i_{ep} multiplied by the pore density N_{ep} . The main drawback of the model is its complexity since several parameters, such as the pore

radius or the relative entrance length of the pore, appearing in the equation cannot be measured and the mathematical well-posedness of the equations is not clearly established. Therefore the inverse problem that consists in fitting the parameter for each cell species is almost unsolvable. In addition the “philosophy” of the modeling is based on the pore creation, while as hinted above the very existence of these pores is controversial. We eventually would say that the multi-pulses description is not taken into account by these models, in particular no memory effect of the previous pulses are included in the models. For all these reasons we choose to present here a new phenomenological model of electropermeabilization that could be fitted with the experiments, and that could describe the membrane resealing and the memory of the applied pulses.

Our electropermeabilization modeling consists in describing the membrane permeabilization by choosing an appropriate function for the surface conductivity S_m , instead of adding an electroporation current based on the pore creation as Krassowska, Neu *et al.* did (see [14, 3, 15]). In addition we propose two models: the first one is a “static” model that describes the electropermeabilization as being an instantaneous phenomenon for a single time-constant pulse. This can be seen as a preliminary model that describes the cell potential during the pulse. The second model is the time-dependent model of electropermeabilization. For each model, we present the theoretical results that ensure existence and uniqueness of the solution to the new problems and then we present the numerical methods that allow the numerical computation of the equations. We conclude by presenting numerical comparisons with the Neu and Krassowska’s model.

2 The static equation

Let σ be the conductivity of the medium, that is

$$\sigma = \begin{cases} \sigma_e, & \text{in the exterior domain } \mathcal{O}_e, \\ \sigma_c, & \text{inside the cell } \mathcal{O}_c. \end{cases}$$

Based on the extensive review of Ivorra *et al* [10], the surface conductivity S_m is a function of the absolute membrane potential, which tends to the value S_L (the lipid surface conductivity) below a certain threshold V_{rev} (the reversible electropermeabilization voltage) and tends to S_{ir} (the surface conductivity of the irreversibly electropermeabilized region) above that threshold, with S_{ir} being larger than S_L . The “speed of the switch” between these two values is given by a parameter k_{ep} . We may choose the following sigmoid function for S_m :

$$\forall \lambda \in \mathbb{R}, \quad S_m(\lambda) = S_L + (S_{ir} - S_L)[1 + \tanh(k_{ep}(|\lambda| - V_{rev}))]/2 \quad (2)$$

however other functions with similar monotonicity properties can be considered, more precisely the function S_m will satisfy the following condition:

$$\left. \begin{aligned} S_m &\in C(\mathbb{R}), \lambda \mapsto S_m(\lambda) \text{ is even on } \mathbb{R}, \\ 0 &< S_L \leq S_m(\lambda) \leq S_{ir}, \quad S_m \text{ is non decreasing on } [0, +\infty), \\ \lim_{\lambda \rightarrow +\infty} S_m(\lambda) &= S_{ir}. \end{aligned} \right\} \quad (3)$$

In particular note that the mapping $\lambda \mapsto \lambda S_m(\lambda)$ is increasing on \mathbb{R} .

Thus we consider that the static potential U satisfies the following problem:

$$\Delta U = 0, \quad \text{in } \mathcal{O}_e \cup \mathcal{O}_c, \quad (4a)$$

$$[\sigma \partial_{\mathbf{n}} U]_{\Gamma} = 0, \quad \text{on } \Gamma \quad (4b)$$

$$S_m([U]_{\Gamma}) [U]_{\Gamma} = \sigma_c \partial_{\mathbf{n}} U|_{\Gamma^-}, \quad \text{on } \partial\Omega \quad (4c)$$

$$U = g \quad \text{on } \partial\Omega. \quad (4d)$$

Remark 2.1. Model (4) can be seen as the limit of the model of Ivorra et al. [10], when the membrane thickness tends to zero (we refer to [18] for asymptotic expansion of the voltage potential in high contrast medium with resistive thin layer).

In the following subsections, we study this non-linear problem. In particular, we emphasize that due to the non-linearity of the membrane conductivity, any numerical membrane widening as performed in [10] leads to irrelevant results from the quantitative point of view. Therefore we aim at providing efficient numerical methods in order to solve the above problem.

2.1 Existence and uniqueness of the static potential

In this subsection we prove the following theorem.

Theorem 2.2. Let $g \in H^{1/2}(\partial\Omega)$. There exists a unique U satisfying problem (4). This solution satisfies

$$U|_{\mathcal{O}_e} \in H^1(\mathcal{O}_e), \quad U|_{\mathcal{O}_c} \in H^2(\mathcal{O}_c).$$

In order to prove this theorem, we proceed as follows. Denote by Λ_c and Λ_e the Dirichlet-to-Neumann operators on Γ (also called Steklov-Poincaré operators) for the Laplacian respectively in \mathcal{O}_c and in \mathcal{O}_e . More precisely, denote by \mathbf{n}_c (respectively \mathbf{n}_e) the unitary outward normal to Γ directed from the interior to the exterior of \mathcal{O}_c (respectively exterior of \mathcal{O}_e). For a function f defined on Γ , we define:

$$\Lambda_c(f) := \mathbf{n}_c \cdot \sigma_c \nabla v_{c|_{\Gamma^-}}, \quad \text{where } \operatorname{div}(\sigma_c \nabla v_c) = 0 \text{ in } \mathcal{O}_c, \text{ and } v_{c|_{\Gamma}} = f, \quad (5a)$$

$$\Lambda_e(f) := \mathbf{n}_e \cdot \sigma_e \nabla v_{e|_{\Gamma^+}}, \quad \text{where} \\ \operatorname{div}(\sigma_e \nabla v_e) = 0 \text{ in } \mathcal{O}_e, \quad v_{e|_{\partial\Omega}} = 0 \text{ and } v_{e|_{\Gamma}} = f. \quad (5b)$$

Observe that using the Wirtinger–Poincaré’s inequality in the case of Λ_c , or Poincaré’s inequality in the case of Λ_e , together with the continuity of the mapping $u \mapsto u|_{\partial\mathcal{O}}$ from $H^1(\mathcal{O})$ into $H^{1/2}(\partial\mathcal{O})$ when \mathcal{O} is sufficiently smooth, we have that

$$\langle \Lambda_c f, f \rangle = \int_{\mathcal{O}_c} \sigma_c(x) \nabla v_c(x) \cdot \nabla v_c(x) dx \geq C_c \|f - M(f)\|_{H^{1/2}(\Gamma)}^2, \quad (6)$$

$$\langle \Lambda_e f, f \rangle = \int_{\mathcal{O}_e} \sigma_e(x) \nabla v_e(x) \cdot \nabla v_e(x) dx \geq C_e \|f\|_{H^{1/2}(\Gamma)}^2, \quad (7)$$

where $M(f) = |\Gamma|^{-1} \int_{\Gamma} f(\tau) d\tau$ is the mean value of f on Γ , and C_e and C_c are constants depending only on \mathcal{O}_e and \mathcal{O}_c respectively. Moreover, for a function $g \in H^{1/2}(\partial\Omega)$, we define $\Lambda_0(g)$ by:

$$\Lambda_0(g) := \mathbf{n}_e \cdot \sigma_e \nabla v|_{\Gamma^+}, \quad \text{where} \\ \operatorname{div}(\sigma_e \nabla v) = 0 \text{ in } \mathcal{O}_e, \quad v|_{\partial\Omega} = g \text{ and } v|_{\Gamma} = 0. \quad (8)$$

It is useful to recall that the operator Λ_e is invertible, its inverse being given by another Steklov-Poincaré operator (or what is sometimes called a Neumann-to-Dirichlet operator), namely for $\psi \in H^{-1/2}(\Gamma)$ given one has $\Lambda_e^{-1}(\psi) = v|_{\Gamma}$ where $v \in H^1(\mathcal{O}_e)$ satisfies the equation

$$\operatorname{div}(\sigma_e \nabla v) = 0 \text{ in } \mathcal{O}_e, \quad v|_{\partial\Omega} = 0 \text{ and } \mathbf{n}_e \cdot \sigma_e \nabla v|_{\Gamma^+} = \psi.$$

Consider the Hilbert space \mathbb{H} defined by

$$\mathbb{H} = H^{1/2}(\Gamma) \times H^{1/2}(\Gamma),$$

with the norm

$$\forall \mathbf{u} = (u_e, u_c) \in \mathbb{H}, \quad \|\mathbf{u}\|_{\mathbb{H}}^2 = \|u_e\|_{H^{1/2}(\Gamma)}^2 + \|u_c\|_{H^{1/2}(\Gamma)}^2.$$

Problem (4) can be written on the manifold Γ with the help of the above Steklov-Poincaré operators: more precisely problem (4) is equivalent to finding $(u_e, u_c) \in \mathbb{H}$ such that

$$\begin{aligned} \Lambda_e u_e + S_m(u_e - u_c)(u_e - u_c) &= -\Lambda_0(g), \\ \Lambda_c u_c - S_m(u_e - u_c)(u_e - u_c) &= 0. \end{aligned} \tag{9}$$

The proof of Theorem 2.2 is an obvious application of the following theorem.

Theorem 2.3. *Let $\mathbf{G} = (G_e, G_c) \in \mathbb{H}'$. There exists a unique $\mathbf{u}^0 = (u_e, u_c) \in \mathbb{H}$ such that*

$$\begin{aligned} \Lambda_e u_e + S_m(u_e - u_c)(u_e - u_c) &= G_e, \\ \Lambda_c u_c - S_m(u_e - u_c)(u_e - u_c) &= G_c. \end{aligned} \tag{10}$$

Proof. We denote by \mathbb{H}' the dual space of \mathbb{H} and by $\langle \cdot, \cdot \rangle$ the duality between \mathbb{H} and \mathbb{H}' . We define the operator Λ_σ from \mathbb{H} into \mathbb{H}' by

$$\forall \mathbf{u} \in \mathbb{H}, \quad \Lambda_\sigma \mathbf{u} = \begin{pmatrix} \Lambda_e u_e \\ \Lambda_c u_c \end{pmatrix} = \begin{pmatrix} \Lambda_e & 0 \\ 0 & \Lambda_c \end{pmatrix} \begin{pmatrix} u_e \\ u_c \end{pmatrix} \tag{11}$$

Observe that thanks to (6) and (7) we have

$$\forall \mathbf{u} \in \mathbb{H}, \quad \langle \Lambda_\sigma \mathbf{u}, \mathbf{u} \rangle \geq C_e \|u_e\|_{H^{1/2}(\Gamma)}^2 + C_c \|u_c - M(u_c)\|_{H^{1/2}(\Gamma)}^2. \tag{12}$$

The function S_m satisfying conditions (3), introduce the function F defined by

$$\forall s \in \mathbb{R}, \quad F(s) = \int_0^s S_m(z) z \, dz,$$

note that F is even, that is $F(-s) = F(s)$. Let \mathbf{J}_1 be the function defined on \mathbb{H} by

$$\forall \mathbf{u} \in \mathbb{H}, \quad \mathbf{J}_1(\mathbf{u}) = \mathbf{J}_1(u_e, u_c) = \int_{\Gamma} F(u_e(\tau) - u_c(\tau)) d\tau,$$

one easily checks that \mathbf{J}_1 is a C^1 function on \mathbb{H} and

$$J_1(\mathbf{u}) \geq \frac{1}{2} S_L \int_{\Gamma} |u_e(\tau) - u_c(\tau)|^2 d\tau$$

Observe that for any $\mathbf{u} \in \mathbb{H}$, the linear map $\mathbf{J}'_1(\mathbf{u})$ is defined by

$$\forall (\mathbf{u}, \mathbf{h}) \in \mathbb{H}^2, \quad \mathbf{J}'_1(\mathbf{u}) \cdot \mathbf{h} = \int_{\Gamma} S(u_e(\tau) - u_c(\tau))(u_e(\tau) - u_c(\tau))(h_e(\tau) - h_c(\tau)) d\tau.$$

Let \mathbf{J} be defined by

$$\forall \mathbf{u} \in \mathbb{H}, \quad \mathbf{J}(\mathbf{u}) = \frac{1}{2} \langle \Lambda_\sigma \mathbf{u}, \mathbf{u} \rangle + \mathbf{J}_1(\mathbf{u}) - \langle \mathbf{G}, \mathbf{u} \rangle.$$

\mathbf{J} is of class \mathcal{C}^1 on \mathbb{H} and \mathbf{J}' is given by

$$\forall \mathbf{u} \in \mathbb{H}, \quad \mathbf{J}'(\mathbf{u}) = \begin{pmatrix} \Lambda_e u_e + S_m(u_e - u_c)(u_e - u_c) - G_e \\ \Lambda_c u_c - S_m(u_e - u_c)(u_e - u_c) - G_c \end{pmatrix}. \tag{13}$$

In order to show that \mathbf{J}' is a monotone operator, we define the nonlinear operator B from \mathbb{H}^2 into \mathbb{R} by

$$\forall(\mathbf{u}, \mathbf{v}) \in \mathbb{H}^2, \quad B(\mathbf{u}, \mathbf{v}) = S_m([\mathbf{u}])[\mathbf{u}]^2 \left(1 - \frac{[\mathbf{v}]}{[\mathbf{u}]}\right) \left(1 - \frac{S_m([\mathbf{v}])[\mathbf{v}]}{S_m([\mathbf{u}])[\mathbf{u}]}\right), \quad (14)$$

where for simplicity we denote by $[\mathbf{u}] = u_e - u_c$ for $\mathbf{u} = (u_e, u_c) \in \mathbb{H}$. Taking into account the fact that S_m satisfies (3), one checks easily that $B(\mathbf{u}, \mathbf{v}) \geq 0$. According to (12) and (13), for $(\mathbf{u}, \mathbf{v}) \in \mathbb{H}^2$ we have

$$\langle \mathbf{J}'(\mathbf{u}) - \mathbf{J}'(\mathbf{v}), \mathbf{u} - \mathbf{v} \rangle = \langle \Lambda_\sigma(\mathbf{u} - \mathbf{v}), \mathbf{u} - \mathbf{v} \rangle + \int_\Gamma B(\mathbf{u}(s), \mathbf{v}(s)) ds, \quad (15)$$

from which we infer that \mathbf{J}' is a monotone operator. Therefore \mathbf{J} is convex. In order to see the strict convexity of \mathbf{J} , that is the strict monotonicity of \mathbf{J}' , we have to show that for if a given $\mathbf{u}, \mathbf{v} \in \mathbb{H}$ we have $\langle \mathbf{J}'(\mathbf{u}) - \mathbf{J}'(\mathbf{v}), \mathbf{u} - \mathbf{v} \rangle = 0$, we have $\mathbf{u} = \mathbf{v}$. First observe that since $\lambda \mapsto \lambda S_m(\lambda)$ is increasing, we have that

$$B(\mathbf{u}, \mathbf{v}) = 0 \quad \implies \quad [\mathbf{u}] = [\mathbf{v}].$$

So for these \mathbf{u}, \mathbf{v} we have in particular $B(\mathbf{u}, \mathbf{v}) = 0$, which implies $[\mathbf{u}] = [\mathbf{v}]$, that is $u_e - v_e = u_c - v_c$. On the other hand, since

$$\langle \Lambda_e(u_e - v_e), u_e - v_e \rangle = \langle \Lambda_c(u_c - v_c), u_c - v_c \rangle = 0,$$

and since Λ_e is coercive, we conclude that $u_e - v_e = 0$, which in turn implies that $u_c - v_c = 0$. Finally this shows that

$$\langle \mathbf{J}'(\mathbf{u}) - \mathbf{J}'(\mathbf{v}), \mathbf{u} - \mathbf{v} \rangle = 0 \quad \implies \quad \mathbf{u} = \mathbf{v},$$

that is that \mathbf{J}' is strictly monotone and \mathbf{J} is strictly convex.

In order to show the coerciveness of \mathbf{J} , that is $\mathbf{J}(\mathbf{u}) \rightarrow +\infty$ when $\|\mathbf{u}\|_{\mathbb{H}} \rightarrow \infty$, we proceed as follows. Observe first that

$$\begin{aligned} |\langle G_c, M(u_c) \rangle| &\leq \|G_c\|_{H^{-1/2}(\Gamma)} \|M(u_e - u_c)\|_{H^{1/2}(\Gamma)} \\ &\quad + \|G_c\|_{H^{-1/2}(\Gamma)} \|M(u_e)\|_{H^{1/2}(\Gamma)}, \\ &\leq \|G_c\|_{H^{-1/2}(\Gamma)} \|M(u_e - u_c)\|_{H^{1/2}(\Gamma)} \\ &\quad + \|G_c\|_{H^{-1/2}(\Gamma)} \|u_e\|_{H^{1/2}(\Gamma)}, \end{aligned}$$

hence

$$\begin{aligned} |\langle \mathbf{G}, \mathbf{u} \rangle| &\leq \left(\|G_e\|_{H^{-1/2}(\Gamma)} + \|G_c\|_{H^{-1/2}(\Gamma)} \right) \|u_e\|_{H^{1/2}(\Gamma)} \\ &\quad + \|G_c\|_{H^{-1/2}(\Gamma)} \|u_c - M(u_c)\|_{H^{1/2}(\Gamma)} \\ &\quad + \|G_c\|_{H^{-1/2}(\Gamma)} \|M(u_e - u_c)\|_{H^{1/2}(\Gamma)}, \end{aligned}$$

using Young's inequality ($ab \leq \varepsilon a^2 + C(\varepsilon)b^2$, for $\varepsilon > 0$ and $C(\varepsilon) := (4\varepsilon)^{-1}$) we infer

$$\begin{aligned} |\langle \mathbf{G}, \mathbf{u} \rangle| &\leq \varepsilon \|u_e\|_{H^{1/2}(\Gamma)}^2 + \varepsilon \|u_c - M(u_c)\|_{H^{1/2}(\Gamma)}^2 + C(\varepsilon) \|\mathbf{G}\|_{\mathbb{H}'}^2 \\ &\quad + \|G_c\|_{H^{-1/2}(\Gamma)} \|M(u_e - u_c)\|_{H^{1/2}(\Gamma)}. \end{aligned} \quad (16)$$

On the other hand using the fact that $2F(s) \geq S_L s^2$ for $s \in \mathbb{R}$, we deduce that

$$\begin{aligned} \mathbf{J}_1(\mathbf{u}) &\geq \frac{1}{2} S_L \int_{\Gamma} |u_e(\tau) - u_c(\tau)|^2 d\tau \\ &\geq \frac{1}{2} S_L \left(\int_{\Gamma} |(u_e - u_c) - M(u_e - u_c)|^2 d\tau + \int_{\Gamma} |M(u_e - u_c)|^2 d\tau \right). \end{aligned}$$

Using this, together with (16), we obtain a lower bound for $\mathbf{J}(\mathbf{u})$ (here $a(\varepsilon), C(\varepsilon)$ are positive constants depending on the arbitrary $\varepsilon > 0$, and $b > 0$ is a constant):

$$\begin{aligned} \mathbf{J}(\mathbf{u}) &\geq a(\varepsilon) \left(\|u_e\|_{H^{1/2}(\Gamma)}^2 + \|u_c - M(u_c)\|_{H^{1/2}(\Gamma)}^2 \right) \\ &\quad + b \int_{\Gamma} |M(u_e - u_c)|^2 d\tau - \|G_c\|_{H^{-1/2}(\Gamma)} \|M(u_e - u_c)\|_{H^{1/2}(\Gamma)} \\ &\quad - C(\varepsilon) \|\mathbf{G}\|_{\mathbb{H}'}^2. \end{aligned} \tag{17}$$

Since $M(u_e - u_c)$ is a constant, we observe that for some positive constant c_* independent of \mathbf{u} one has $\|M(u_e - u_c)\|_{H^{1/2}(\Gamma)} = c_* \|M(u_e - u_c)\|_{L^2(\Gamma)}$, and consequently for any $\varepsilon > 0$ so that $b - \varepsilon > 0$, there exists a constant $c(\varepsilon)$ such that

$$\begin{aligned} b \int_{\Gamma} |M(u_e - u_c)|^2 d\tau - \|G_c\|_{H^{-1/2}(\Gamma)} \|M(u_e - u_c)\|_{H^{1/2}(\Gamma)} &\geq \\ (b - \varepsilon) \|M(u_e - u_c)\|_{H^{1/2}(\Gamma)}^2 - c(\varepsilon) \|G_c\|_{H^{-1/2}(\Gamma)}^2. \end{aligned}$$

Using this in the lower bound (17) we conclude that

$$\lim_{\|\mathbf{u}\|_{\mathbb{H}} \rightarrow +\infty} \mathbf{J}(\mathbf{u}) = +\infty$$

hence \mathbf{J} achieves its minimum at a unique point $\mathbf{u}^0 \in \mathbb{H}$, which satisfies equation (10). \square

3 The dynamical model

In this section we focus on the dynamical description of the electropermeabilization. Our model is based on the description of two quantities: the time-dependent electric potential and the ratio of the electropermeabilized region over the total membrane area, which is also time-dependent. We present in subsection 3.1 the main considerations that lead to our model, and then we study its solvability: existence and uniqueness results are presented in subsection 3.4.

3.1 Heuristics of the modeling

Experimental observations suggest that the permeabilization process at a certain location depends on whether the membrane conductivity is above a certain threshold or not. This leads us to define the surface membrane conductivity as an interpolation between the two values S_{ir} and S_L , the interpolation parameter $\xi(t, s) \in [0, 1]$ being itself a function of time and of the point s on the membrane Γ . In our interpretation the parameter $\xi(t, s)$ measures in some way the likelihood that a given infinitesimal portion of the membrane is going to be electropermeabilized. More precisely, when $\xi(t, s)$ equals 0 at a given point $s \in \Gamma$, the membrane conductivity equals the lipid conductivity at this point (thus there is no electropermeabilization), while for $\xi(t, s) = 1$ it corresponds to the *pore* conductivity (hence there is electropermeabilization). Thus we set:

$$\forall (t, s) \in (0, \infty) \times \Gamma, \quad S_m(t, s) = S_L + \xi(t, s)(S_{\text{ir}} - S_L). \tag{18}$$

On the other hand since the changes in the conductivity at a certain location $s \in \Gamma$ depend on the transmembrane potential, denoting by $[\mathbf{u}] := u_e - u_c$ the *jump* in the potential between the exterior and the interior of the cell for $\mathbf{u} := (u_e, u_c) \in \mathbb{H}$ (as we did in the previous sections), in the model studied here we assume that

$$\xi(t, s) = X(t, [\mathbf{u}(t, s)]), \quad (19)$$

where the function $(t, \lambda) \mapsto X(t, \lambda)$ will be defined below.

The main idea of the model we present here consists in writing a differential equation that describes the dynamics of $(t, \lambda) \mapsto X(t, \lambda)$, similarly to a *sliding door* model, as follows. Let β be a function satisfying

$$\left. \begin{array}{l} \beta \in W^{1,\infty}(\mathbb{R}), \lambda \mapsto \beta(\lambda) \text{ is even on } \mathbb{R}, \\ 0 \leq \beta(\lambda) \leq 1, \quad \beta \text{ is non decreasing on } [0, +\infty), \\ \lim_{\lambda \rightarrow +\infty} \beta(\lambda) = 1. \end{array} \right\} \quad (20)$$

An example of such a function would be

$$\forall \lambda \in \mathbb{R}, \quad \beta(\lambda) := (1 + \tanh(k_{\text{ep}}(|\lambda| - V_{\text{rev}})))/2.$$

Now for $\lambda_0 \in \mathbb{R}$ (which is going to denote the potential jump $[\mathbf{u}(t_0, s)]$) let $X_0(\lambda_0) \in [0, 1]$ be the initial value of $X(\cdot, \lambda_0)$ at time t_0 . When a cell is at rest, X_0 equals zero, but if high voltage pulses have been applied earlier than the initial time, X_0 might not be equal to zero. At the time t_0 , consider the jump of the potential $\lambda_0 := [\mathbf{u}(t_0, s)]$ and set $\beta_0 := \beta(\lambda_0)$. Then there are two possibilities:

- Either $\beta_0 - X_0$ is positive, in which case the electric pulse is sufficiently high to enlarge the electropermeabilized region, with a *characteristic time of electropermeabilization* of order τ_{ep} .
- Or $\beta_0 - X_0$ is negative, and therefore the pulse is not high enough to increase the electropermeabilization. Therefore, the membrane *tries to reseal* with a characteristic *resealing* time of order τ_{res} . Since experimental observations suggest that this phenomenon takes much more time than the electropermeabilization process, we assume that $\tau_{\text{res}} > \tau_{\text{ep}}$.

Based on these considerations, $t \mapsto \lambda(t)$ being a given function of time (actually $\lambda(t)$ is going to be $[\mathbf{u}(t, s)]$, see below for the type of regularity needed) we assume that X satisfies the following differential equation:

$$\begin{cases} \frac{\partial X}{\partial t}(t, \lambda) = \max\left(\frac{\beta(\lambda(t)) - X(t, \lambda)}{\tau_{\text{ep}}}; \frac{\beta(\lambda(t)) - X(t, \lambda)}{\tau_{\text{res}}}\right), \\ X(0, \lambda) = X_0(\lambda(0)). \end{cases} \quad (21)$$

Observe that when $\lambda(t) := \lambda(t, s) := [\mathbf{u}(t, s)]$, if \mathbf{u} and X are stabilized at their respective stationary values $\mathbf{u}^*(s)$ and $X^*(\lambda(\cdot, s))$, then the unique stationary solution of the above equation is given by

$$X^*(\lambda(\cdot, s)) = \beta([\mathbf{u}^*(s)]),$$

and taking definition (19) into account, equality (18) becomes

$$S_m^*(s) = S_L + (S_{\text{ir}} - S_L)\beta([\mathbf{u}^*(s)])$$

which coincides with the definition of the static membrane conductivity (2), in which one may have for instance a particular choice

$$\beta(\lambda) := (1 + \tanh(k_{\text{ep}}(|\lambda| - V_{\text{rev}})))/2.$$

As we shall see below, this interpretation of the model and the numerical simulations we present below agree with some experimental data existing in the literature.

3.2 Statement of the mathematical problem

First we write the problem satisfied by the potential U defined on the domain $\mathcal{O}_e \times \mathcal{O}_c$, assuming that before the imposition of the electrical pulses g , on the external boundary $\partial\Omega$, the cell potential is at rest given by $U_0 \in H^1(\Omega)$, that translates the ionic exchanges through the membrane. A function \tilde{S}_m is defined through equality (18) and (19) by:

$$\tilde{S}_m(t, \lambda) := S_L + (S_{\text{ir}} - S_L)X(t, \lambda) \quad (22)$$

We seek the solution (U, X) to the following system of equations:

$$\Delta U = 0, \quad \text{in } (0, T) \times (\mathcal{O}_e \cup \mathcal{O}_i), \quad (23a)$$

$$[\sigma \partial_{\mathbf{n}} U] = 0, \quad \text{on } (0, T) \times \Gamma, \quad (23b)$$

$$C_m \partial_t [U](t, \cdot) + \tilde{S}_m(t, [U])[U] = \sigma_i \partial_{\mathbf{n}} U(t, \cdot)|_{\Gamma^-}, \quad \text{on } (0, T) \times \Gamma, \quad (23c)$$

$$U(t, \cdot) = g(t, \cdot) \quad \text{on } (0, +\infty) \times \partial\Omega, \quad (23d)$$

$$U(0, \cdot) = U_0 \quad \text{in } \mathcal{O}_e \cup \mathcal{O}_c, \quad (23e)$$

where the function X appearing in (22) satisfies the differential equation for $t > 0$ (here we set $\lambda(t) := \lambda(t, s) := [U(t, s)]$ for a.e. $s \in \Gamma$):

$$\begin{cases} \frac{\partial X(t, \lambda)}{\partial t} = \max \left(\frac{\beta(\lambda(t)) - X(t, \cdot)}{\tau_{\text{ep}}}; \frac{\beta(\lambda(t)) - X(t, \cdot)}{\tau_{\text{res}}} \right), \\ X(0, \lambda) = 0. \end{cases} \quad (24)$$

3.3 Resolution of the differential equation (24)

Here we state the following lemma regarding the solution of equation (24):

Lemma 3.1. *Let $T > 0$ be fixed and let β satisfy condition (20). For any $\lambda \in L^p(0, T)$, with $1 \leq p \leq \infty$, the following differential equation for $t \in (0, T)$*

$$\begin{cases} \frac{\partial X(t, \lambda)}{\partial t} = \max \left(\frac{\beta(\lambda(t)) - X(t, \lambda)}{\tau_{\text{ep}}}; \frac{\beta(\lambda(t)) - X(t, \lambda)}{\tau_{\text{res}}} \right), \\ X(0, \lambda) = X_0 \in [0, 1], \end{cases} \quad (25)$$

has a unique solution $X(\cdot, \lambda) \in W^{1,p}(0, T)$. Moreover $0 \leq X(t, \lambda) \leq 1$ for all $t \in [0, T]$, while $X(\cdot, \lambda) = X(\cdot, -\lambda) = X(\cdot, |\lambda|)$ and there exists a constant $K(T) > 0$ depending on $\|\beta'\|_\infty$ such that for $\lambda_1, \lambda_2 \in L^p(0, T)$ with $1 \leq p \leq \infty$, we have

$$\|X(\cdot, \lambda_1) - X(\cdot, \lambda_2)\|_{L^\infty(0, T)} \leq K(T) \|\lambda_1 - \lambda_2\|_{L^p(0, T)}. \quad (26)$$

More precisely the constant $K(T)$ is given by

$$K(T) = T^{(p-1)/p} \|\beta'\|_\infty \exp(\max(\tau_{\text{ep}}^{-1}, \tau_{\text{res}}^{-1})T).$$

Proof. The mapping $X \mapsto \max([\beta(\lambda(t)) - X]/\tau_{\text{ep}}, [\beta(\lambda(t)) - X]/\tau_{\text{res}})$ is clearly Lipschitz for all fixed t , while

$$t \mapsto \max([\beta(\lambda(t)) - X]/\tau_{\text{ep}}, [\beta(\lambda(t)) - X]/\tau_{\text{res}})$$

is in $L^p(0, T)$ for all fixed X . Therefore the differential equation (25) has a unique solution $X \in W^{1,p}(0, T)$, for any $X_0 \in \mathbb{R}$.

Now assuming that $0 \leq X_0 \leq 1$, multiplying the equation (25) by $X^- := \max(-X, 0)$, and using the fact that $\beta \geq 0$, one gets

$$\frac{1}{2} \partial_t |X^-|^2 \leq 0,$$

thus $X^-(t, \lambda) \equiv 0$ on $[0, T]$. Similarly, using the fact that $\beta - 1 \leq 0$, multiplying the equation by $(X - 1)^+ = \max(X - 1, 0)$ one sees that

$$\partial_t |(X - 1)^+|^2 \leq 0,$$

and finally $0 \leq X(t, \lambda) \leq 1$.

In order to prove the Lipschitz continuous dependence of X on λ , note that setting

$$F(\lambda, X) := \max\left(\frac{\beta(\lambda(\cdot)) - X}{\tau_{\text{ep}}}; \frac{\beta(\lambda(\cdot)) - X}{\tau_{\text{res}}}\right), \quad (27)$$

and denoting by $X_j := X(\cdot, \lambda_j)$ for $j = 1, 2$, the respective solutions to (25), we have $\partial_t (X_1 - X_2) = F(\lambda_1, X_1) - F(\lambda_2, X_2)$, and thus

$$X_1(t) - X_2(t) = \int_0^t (F(\lambda_1, X_1) - F(\lambda_2, X_2))(s) ds.$$

Now note that we may write

$$F(\lambda_1, X_1) - F(\lambda_2, X_2) = [F(\lambda_1, X_1) - F(\lambda_2, X_1)] + [F(\lambda_2, X_1) - F(\lambda_2, X_2)],$$

and that for $0 \leq s \leq t \leq T$ we have

$$\begin{aligned} \|F(\lambda_1, X_1) - F(\lambda_2, X_1)\|_{L^p(0,t)} &\leq \|\beta'\|_{\infty} \|\lambda_1 - \lambda_2\|_{L^p(0,t)}, \\ |(F(\lambda_2, X_1) - F(\lambda_2, X_2))(s)| &\leq \max(1/\tau_{\text{ep}}, 1/\tau_{\text{res}}) |X_1(s) - X_2(s)|. \end{aligned}$$

Thus using the fact that by Hölder's inequality

$$\begin{aligned} \int_0^t |(F(\lambda_1, X_1) - F(\lambda_2, X_1))(s)| ds &\leq t^{(p-1)/p} \|F(\lambda_1, X_1) - F(\lambda_2, X_1)\|_{L^p(0,t)}, \\ &\leq T^{(p-1)/p} \|\beta'\|_{\infty} \|\lambda_1 - \lambda_2\|_{L^p(0,T)}, \end{aligned}$$

we infer that the following inequality holds for $|X_1(t) - X_2(t)|$

$$\begin{aligned} |X_1(t) - X_2(t)| &\leq T^{(p-1)/p} \|\beta'\|_{\infty} \|\lambda_1 - \lambda_2\|_{L^p(0,T)} \\ &\quad + \max(1/\tau_{\text{ep}}, 1/\tau_{\text{res}}) \int_0^t |X_1(s) - X_2(s)| ds, \end{aligned}$$

which yields the estimate (26), thanks to Gronwall's lemma. \square

Remark 3.2. *The results of the above lemma are still valid if one replaces $\beta : \mathbb{R} \rightarrow \mathbb{R}$ satisfying (20) with a function $\beta \in L^\infty((0, T) \times \mathbb{R})$ such that almost every $t \in (0, T)$, the function $\beta(t, \cdot)$ satisfies (20).*

3.4 Existence and uniqueness

Since the non-linearity of problem (23) appears in the transmission condition (23c), in order to study the problem, we are going to rewrite the problem as a non-linear problem on the surface Γ using the Steklov-Poincaré operators, in the same manner as we did in the previous section for the static model. We first prove the following property:

Lemma 3.3. *The operator $\Lambda_e + \Lambda_c$ is positive, selfadjoint and invertible from $H^{1/2}(\Gamma)$ into $H^{-1/2}(\Gamma)$, and therefore the operator*

$$\mathcal{B} := \text{Id} + \Lambda_e^{-1} \Lambda_c$$

is also invertible, from $H^{1/2}(\Gamma)$ into itself.

Moreover, define the domain $D(\Lambda_c \mathcal{B}^{-1})$ as

$$D(\Lambda_c \mathcal{B}^{-1}) = \left\{ \phi \in H^{1/2}(\Gamma) : \Lambda_c \mathcal{B}^{-1} \phi \in L^2(\Gamma) \right\}.$$

The operator $(\Lambda_c \mathcal{B}^{-1}, D(\Lambda_c \mathcal{B}^{-1}))$ is m -accretive (more precisely $D(\Lambda_c \mathcal{B}^{-1}) = H^1(\Gamma)$).

Proof. That $\Lambda_e + \Lambda_c$ is invertible is an easy consequence of the fact that the operator Λ_e is a positive, selfadjoint and invertible operator while Λ_c is non-negative and selfadjoint. Thus $\Lambda_e + \Lambda_c$ is also a positive selfadjoint invertible operator.

Let $\phi \in D(\Lambda_c \mathcal{B}^{-1})$. Then by definition (and invertibility) of \mathcal{B}

$$\begin{aligned} \langle \Lambda_c \mathcal{B}^{-1} \phi, \phi \rangle &= \langle \Lambda_c \mathcal{B}^{-1} \phi, \phi \rangle, \\ &= \langle \Lambda_c \mathcal{B}^{-1} \phi, \mathcal{B}^{-1} \phi \rangle + \langle \Lambda_c \mathcal{B}^{-1} \phi, \Lambda_e^{-1} \Lambda_c \mathcal{B}^{-1} \phi \rangle, \\ &= \langle \Lambda_c \mathcal{B}^{-1} \phi, \mathcal{B}^{-1} \phi \rangle + \langle \Lambda_e \Lambda_e^{-1} \Lambda_c \mathcal{B}^{-1} \phi, \Lambda_e^{-1} \Lambda_c \mathcal{B}^{-1} \phi \rangle \\ &\geq 0, \end{aligned}$$

hence $\Lambda_c \mathcal{B}^{-1}$ is accretive. Let $f \in L^2(\Gamma)$, let $\lambda > 0$ and let U be the unique solution in $PH_0^1(\Omega)$ to the following problem:

$$\begin{aligned} -\Delta U &= 0, \text{ in } \mathcal{O}_e \cup \mathcal{O}_c, \quad U|_{\partial\Omega} = 0 \\ \sigma_e \partial_{\mathbf{n}} U|_{\Gamma^+} &= \sigma_c \partial_{\mathbf{n}} U|_{\Gamma^-}, \\ \lambda \sigma_c \partial_{\mathbf{n}} U|_{\Gamma^-} + U|_{\Gamma^-} - U|_{\Gamma^+} &= f. \end{aligned}$$

Therefore, setting $v := U|_{\Gamma^-} - U|_{\Gamma^+}$, we have that v satisfies

$$v + \lambda \Lambda_c \mathcal{B}^{-1} v = f,$$

and thus $\Lambda_c \mathcal{B}^{-1}$ is m -accretive, since furthermore $\Lambda_c \mathcal{B}^{-1}$ being nonnegative we have $\|v\|_{L^2(\Gamma)} \leq \|f\|_{L^2(\Gamma)}$. □

Lemma 3.4. *Finding the solution U to problem (23), if it exists, is equivalent to finding (u_e, u_c) with $u_e = U|_{\Gamma^+}$ and $u_c = U|_{\Gamma^-}$ satisfying:*

$$u_e = u_c - v_c, \tag{28}$$

$$u_c = \mathcal{B}^{-1} (v_c - \Lambda_e^{-1} \Lambda_0 g), \tag{29}$$

where v_c is the solution to

$$\begin{aligned} C_m \partial_t v_c + \Lambda_c \mathcal{B}^{-1} v_c + \tilde{S}_m(t, v_c) v_c &= G, \\ v_c(0, \cdot) &= \phi, \end{aligned} \quad (30)$$

with ϕ and G being defined as

$$\phi = U_{0|\Gamma^+} - U_{0|\Gamma^-}, \quad G := \Lambda_c \mathcal{B}^{-1} \Lambda_e^{-1} \Lambda_0 g,$$

and X satisfying

$$\begin{cases} \lambda(t, \cdot) = v_c, \\ \partial_t X(t, \cdot) = \max \left(\frac{\beta(\lambda(t, \cdot)) - X(t, \lambda)}{\tau_{\text{ep}}}; \frac{\beta(\lambda(t, \cdot)) - X(t, \lambda)}{\tau_{\text{res}}} \right), \\ X(0, \cdot) = 0. \end{cases} \quad (31)$$

Proof. The lemma is a straightforward consequence of the definition of the Steklov-Poincaré operators $\Lambda_i, \Lambda_e, \Lambda_0$ and the invertibility of Λ_e . Indeed, condition (23b), that is the continuity of the flux across Γ , boils down to

$$\Lambda_e u_e + \Lambda_0 g + \Lambda_c u_c = 0,$$

from which we infer thanks to the invertibility of Λ_e , that

$$u_e - u_c = -(\mathcal{B} u_c + \Lambda_e^{-1} \Lambda_0 g) = -v_c.$$

in addition by definition of v_c we have

$$\Lambda_c u_c = \Lambda_c \mathcal{B}^{-1} v_c - \Lambda_c \mathcal{B}^{-1} \Lambda_e^{-1} \Lambda_0 g = \Lambda_c \mathcal{B}^{-1} v_c - G.$$

Then the transmission condition (23c) (multiplied by (-1)) reads (30), provided we recall that β is an even function and that \tilde{S}_m is defined by (22). \square

We show now that the evolution equations appearing in lemma 3.4 have a unique solution.

Lemma 3.5. *Assume that β satisfies (20), $G \in L^p((0, T); L^2(\Gamma))$ for some $p > 1$ and $\phi \in L^2(\Gamma)$ is given. Then there exists a unique function $v_c \in C([0, T]; L^2(\Gamma))$, mild solution to the system*

$$\begin{cases} C_m \partial_t v_c + \Lambda_c \mathcal{B}^{-1} v_c + \tilde{S}_m(t, v_c) v_c = G, \\ \lambda(t, \cdot) = v_c, \\ \partial_t X(t, \cdot) = \max \left(\frac{\beta(\lambda(t, \cdot)) - X(t, \lambda)}{\tau_{\text{ep}}}; \frac{\beta(\lambda(t, \cdot)) - X(t, \lambda)}{\tau_{\text{res}}} \right), \\ X(0, \cdot) = 0, \\ v_c(0) = \phi. \end{cases} \quad (32)$$

Moreover if $\phi \in H^1(\Gamma)$ and $G \in W^{1,1}((0, T); L^2(\Gamma))$, then the above mild solution is a classical solution to (32), in the sense that

$$v_c \in C([0, T]; H^1(\Gamma)) \cap C^1([0, T]; L^2(\Gamma)).$$

Proof. To simplify the notations we denote by \mathcal{A} the operator

$$\mathcal{A} = \frac{1}{C_m} \Lambda_c \mathcal{B}^{-1}.$$

In a first step, we are going to show existence and uniqueness of a mild solution to (32) in $C([0, T]; L^2(\Gamma))$. For a given $v_c \in C([0, T], L^2(\Gamma))$, thanks to lemma 3.1 we know that the solution of

$$\begin{cases} \lambda(t, \cdot) = v_c, \\ \partial_t X(t, \cdot) = \max \left(\frac{\beta(\lambda(t, \cdot)) - X(t, \lambda)}{\tau_{\text{ep}}}; \frac{\beta(\lambda(t, \cdot)) - X(t, \lambda)}{\tau_{\text{res}}} \right) \\ X(0, \cdot) = 0 \end{cases}$$

exists and belongs in particular to $W^{1, \infty}((0, T), L^2(\Gamma))$, that $0 \leq X \leq 1$, and the mapping $v_c \mapsto X$ is Lipschitz: for some constant $C > 0$ and $K(T)$ given by lemma 3.1, if X_j denotes the solution of the above equation for $\lambda_j := v_{i, j}$ (with $j = 1$ or $j = 2$)

$$\begin{aligned} \|X_1 - X_2\|_{L^\infty((0, T); L^2(\Gamma))} &\leq K(T) \|\lambda_1 - \lambda_2\|_{L^2((0, T) \times \Gamma)} \\ &\leq C K(T) \|v_{i, 1} - v_{i, 2}\|_{C([0, T]; L^2(\Gamma))}. \end{aligned}$$

Now upon setting

$$\mathcal{F}(t, v_c) := -\tilde{S}_m(t, v_c) v_c + G,$$

solving equations (32) is equivalent to find $v_c \in C([0, T]; L^2(\Gamma))$ solution to the following equation, which is the mild version of the (32)

$$v_c = e^{-t\mathcal{A}} \phi + \frac{1}{C_m} \int_0^t \exp(-(t-\tau)\mathcal{A}) \mathcal{F}(\tau, v_c(\tau)) d\tau. \quad (33)$$

Now it is clear that thanks to the properties proved in lemma 3.1 for $\lambda \mapsto X(\cdot, \lambda)$, the mapping

$$v_c \mapsto \mathcal{F}(\cdot, v_c)$$

is Lipschitz from the space $\mathbb{E} := C([0, T]; L^2(\Gamma))$ into itself. This means that there exists $K_1 > 0$ such that for $v_c, w_c \in C([0, T]; L^2(\Gamma))$ we have

$$\|\mathcal{F}(\cdot, v_c) - \mathcal{F}(\cdot, w_c)\|_{L^\infty((0, T); L^2(\Gamma))} \leq K_1 \|v_c - w_c\|_{L^\infty((0, T); L^2(\Gamma))}.$$

We shall endow the space \mathbb{E} with the norm

$$\|\psi\|_{\mathbb{E}} := \sup_{t \in [0, T]} e^{-\alpha t} \|\psi(t, \cdot)\|_{L^2(\Gamma)},$$

for some $\alpha > 0$ which will be chosen below. If we set

$$\Phi(U_c)(t) := e^{-t\mathcal{A}} \phi + \frac{1}{C_m} \int_0^t \exp(-(t-\tau)\mathcal{A}) \mathcal{F}(\tau, U_c(\tau)) d\tau,$$

then $\Phi : \mathbb{E} \rightarrow \mathbb{E}$ is a continuous mapping, and we shall check that upon choosing α appropriately it is a strict contraction, thus has a unique fixed point providing the unique solution of (33). Indeed

$$\Phi(U_c)(t) - \Phi(V_c)(t) = \int_0^t \exp\left(-\frac{t-\tau}{C_m} \Lambda_c \mathcal{B}^{-1}\right) [\mathcal{F}(\tau, U_c) - \mathcal{F}(\tau, V_c)] d\tau.$$

Since the operator $\Lambda_c \mathcal{B}^{-1}$ is m -accretive, the operator \mathcal{A} generates a contraction semi-group and the following estimate holds

$$\|e^{-(t-\tau)\mathcal{A}} [\mathcal{F}(\tau, U_c) - \mathcal{F}(\tau, V_c)]\|_{L^2(\Gamma)} \leq \|[\mathcal{F}(\tau, U_c) - \mathcal{F}(\tau, V_c)]\|_{L^2(\Gamma)},$$

and therefore

$$\begin{aligned} \|\Phi(U_c)(t) - \Phi(V_c)(t)\|_{L^2(\Gamma)} &\leq \left\| \int_0^t \|\mathcal{F}(\tau, U_c) - \mathcal{F}(\tau, V_c)\|_{L^2(\Gamma)} d\tau, \right. \\ &\leq K_1 \|U_c - V_c\|_{\mathbb{E}} \int_0^t e^{\alpha\tau} d\tau, \\ &\leq C(p) K_1 \alpha^{-1} e^{\alpha t} \|U_c - V_c\|_{\mathbb{E}}. \end{aligned}$$

From this we conclude that

$$\|\Phi(U_c) - \Phi(V_c)\|_{\mathbb{E}} \leq \alpha^{-1} C(p) K_1 \|U_c - V_c\|_{\mathbb{E}},$$

which implies that for α large enough, the mapping Φ is a strict contraction on \mathbb{E} . Thus equation (32) has a unique mild solution in $C([0, T]; L^2(\Gamma))$.

Suppose now that G belongs to $W^{1,1}([0, T]; L^2(\Gamma))$ and $\phi \in H^1(\Gamma)$. Then the mild solution given by formula (33) belongs to $C^1([0, T]; L^2(\Gamma))$ thus

$$\partial_t v_c + \tilde{S}_m(\cdot, v_c) v_c \in C([0, T]; L^2(\Gamma)).$$

Therefore setting $U_c = U|_{\mathcal{O}_c}$, we have

$$\Delta U_c(t, \cdot) = 0, \text{ in } \mathcal{O}_c, \quad \sigma_c \partial_n U_c(t, \cdot) \in L^2(\Gamma),$$

from which we infer that $U_c(t, \cdot) \in H^{3/2}(\mathcal{O}_c)$ hence we deduce that since the domains are smooth $U_c(t, \cdot)|_{\Gamma^-} \in H^1(\Gamma)$. Similar reasoning for $U_e = U|_{\mathcal{O}_e}$ implies that $U_e(t, \cdot)|_{\Gamma^+} \in H^1(\Gamma)$, and therefore the jump $v_c \in C([0, T]; H^1(\Gamma))$, which ends the proof. \square

4 Numerical simulations

In this section we provide preliminary numerical results that justify the consistency of our new electroporation model. In order to solve both static and dynamical problems we first present the second order finite-difference method on a cartesian grid adapted from the scheme of Cisternino and Weynans [2].

4.1 Spatial discretization

In both static and dynamical problem a special treatment of points neighbouring the interface is needed for Laplace's operator and fluxes computation. Geometrical information on the interface is provided by a level-set method [16], which defines the extra and intracellular domains by the use of a signed distance function φ .

An example of the discretization method is given by Fig. 1. On regular grid points, that are not neighbouring the interface, the Laplacian is discretized with a standard centered second finite difference scheme. A specific five points stencil including interface points is used for neighbouring points, as shown in Fig. 1(a). This stencil involves additionnal unknowns located at the points where the grid and the interface cross.

The normal to the interface $\mathbf{n}(x)$ outwardly directed from the inner to the outer of the cell is directly obtained by computing $\nabla\varphi(x)$.

Fig. 1(b) provides an example of the computation of ∇U . The x -derivative of U can be easily computed at the second order using a three non-equidistant points formula. The y -derivative cannot be obtained in the same way since there are no grid points of the inner domain aligned with the interface point in the y direction. We therefore use a linear combination of the y -derivatives approximated on the points involved in the x -derivative computation. The scheme is stabilized by using a shifted y -stencil if the interface crosses an involved cell grid. The flux on the other side of the interface is similarly discretized.

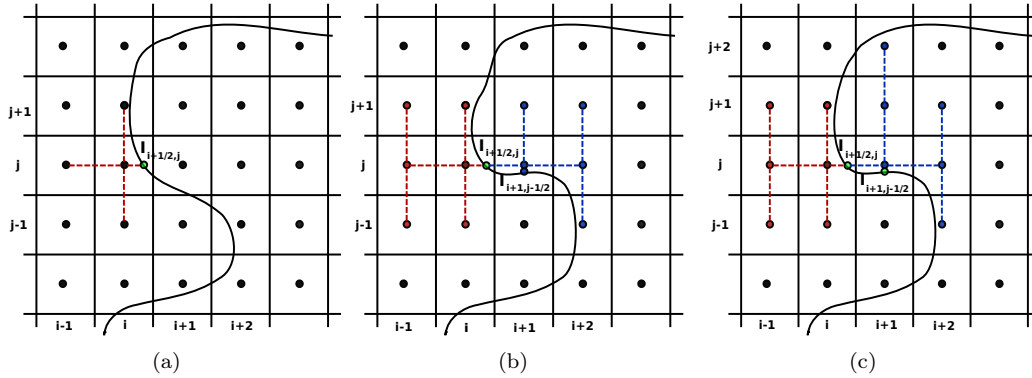


Figure 1: Discretization of the Laplacian on the points at the interface Fig 1(a). Discretization of ∇U on the interface: unstabilized (Fig. 1(b)) and stabilized uncentered stencils (Fig. 1(c)). The first y -derivative stencil on the blue side is shifted to avoid bad conditioning.

4.2 Accuracy of the method

In order to show the accuracy of the numerical method we compare the analytical solution to the numerical solution to the linear model *i.e.* without electroporation.

Actually when the membrane conductivity \tilde{S}_m is fixed to the value S_L , we compute explicitly the solution \bar{U} to the linear problem in the case of concentric circular cell and domain. For a uniform external electric field $g = Er \cos \theta$, the potential has the following form:

$$\bar{U}_e(r, \theta, t) = (\alpha_e(t)r + \beta_e(t)r^{-1}) \cos \theta, \quad \bar{U}_c(r, \theta, t) = \alpha_c(t)r \cos \theta \quad (34)$$

This solution is projected on the edges of our square-shaped computation domain. The error is computed using both grid and interface points :

$$E(\bar{U}, U_h) = \frac{\|U_h - \bar{U}\|_{L^2(\Omega)} + |U_h - \bar{U}|_{L^2(\Gamma)}}{\|\bar{U}\|_{L^2(\Omega)} + |\bar{U}|_{L^2(\Gamma)}} \quad (35)$$

where U_h designates a result obtained on a cartesian grid of pace h . Fig. 2 shows the comparison between this solution and our simulations, confirming the second order of the scheme for the linear case.

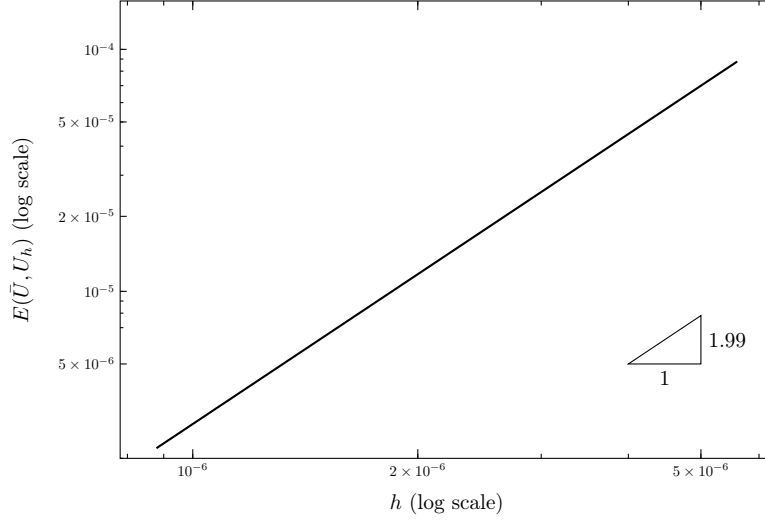


Figure 2: Log-log diagram of the error $E(\bar{U}, U_h)$ given by (35) with respect to h .

4.3 Computation of the non-linear static model

When resolving the static equation (4) using the following naive fixed point method :

$$S_m([U^n])[U^{n+1}] = \sigma_c \partial_{\mathbf{n}} U_c^{n+1}$$

the iterative scheme oscillates between two values, as the membrane conductivity takes its extreme values S_L and S_r instead of reaching an intermediate state. This is due to the fact that the functional \mathcal{L}_g defined by

$$\forall v \in PH^1(\Omega), \quad \mathcal{L}_g(v) = u,$$

where $u \in PH^1(\Omega)$ is solution to

$$\begin{cases} \Delta u = 0, & \text{in } \mathcal{O}_e \cup \mathcal{O}_c, \quad u|_{\partial\Omega} = g, \\ [\sigma \partial_n u]_{\Gamma} = 0, & S_m([v]_{\Gamma})[u]_{\Gamma} = \sigma_c \partial_u|_{\Gamma}, \end{cases}$$

is not contractant, due to the Lipschitz constant of S_m , which is of order $k_{ep} S_m \gg 1$. We use a modified functions $\mathcal{L}_{\rho, g}$ where ρ is a small parameter chosen to ensure the contractility of the functional:

$$\forall v \in PH^1(\Omega), \quad \mathcal{L}_{\rho, g}(v) = u,$$

where $u \in PH^1(\Omega)$ is solution to

$$\begin{cases} \Delta u = 0, & \text{in } \mathcal{O}_e \cup \mathcal{O}_c, \quad u|_{\partial\Omega} = g, \\ [\sigma \partial_n u]_{\Gamma} = 0, & [u]_{\Gamma} + \rho S_m([v]_{\Gamma})[u]_{\Gamma} - \rho \sigma_c \partial_u|_{\Gamma} = [v]_{\Gamma}, \end{cases}$$

hence the following iteration process is used :

$$[U^{n+1}] + \rho S_m([U^n])[U^{n+1}] - \rho \sigma_c \partial_{\mathbf{n}} U_c^{n+1} = [U^n]$$

The stopping criterion of the scheme is set at $\gamma = 10^{-12}$, meaning that numerical solution is obtained when the relative error $E(U^{n+1}, U^n)$ is smaller than γ .

4.3.1 Influence of the parameter S_{ir}

The parameter S_{ir} , which is the conductivity of the fully porated membrane is hardly measurable by the experiments. It is therefore important to investigate its influence on the model. In Fig. 3 we show that S_{ir} has a few influence on the membrane conductivity S_m , as the value of X counter-balance the variation of S_{ir} . Therefore the numerical criterion to define the electroporation should involve the parameter S_m instead of the variable X , which is very sensitive to S_{ir} .

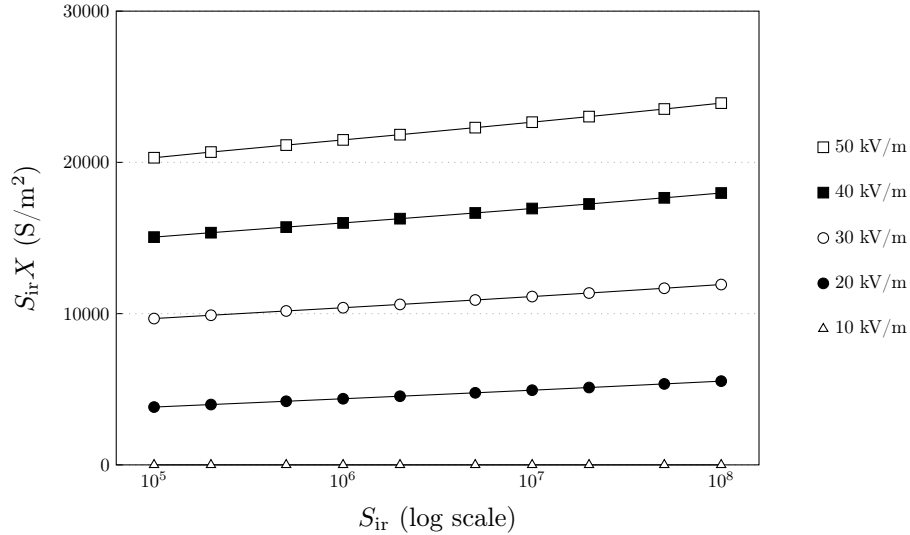


Figure 3: Conductivity of the porated region of the membrane $S_{ir}X$ at the rear pole of the cell ($\theta = 0$) obtained by solving the static equation with different conductivities S_{ir} and pulse magnitudes from 10 to 50 kV/m.

4.3.2 Comparison with the model of Ivorra *et al.*

We compare our results with the simulations of Ivorra *et al.* by studying the influence of the extracellular medium conductivity on the membrane conductivity. In Fig. 4 we show similar qualitative results as the results of Fig. 7 of [10]. Note that to perform their simulations Ivorra *et al.* have widened the membrane thickness ten times larger than its real value, and therefore their permeabilizing field is around 2MV/m of magnitude, which is much larger than the field magnitude used in the experiments. This shortcoming is avoided by our modeling. We emphasize that our results are more accurate since cell electropermeabilization occurs for pulses of magnitude 20-30 kV/m, which is close to the permeabilizing fields observed in the experiments [12, 13, 6].

4.4 The dynamical problem

4.4.1 Time-discretization method of the model

The unstationnary term $C_m \partial_t [U]$ of (23) is discretized using the forward Euler scheme:

$$C_m \frac{[U]^{n+1} - [U]^n}{dt} - \sigma_c \partial_n U_c^{n+1} + \tilde{S}_m ([U]^n) [U]^n = 0 \quad (36)$$

The Runge-Kutta method of order 4 is used to compute the variable X .

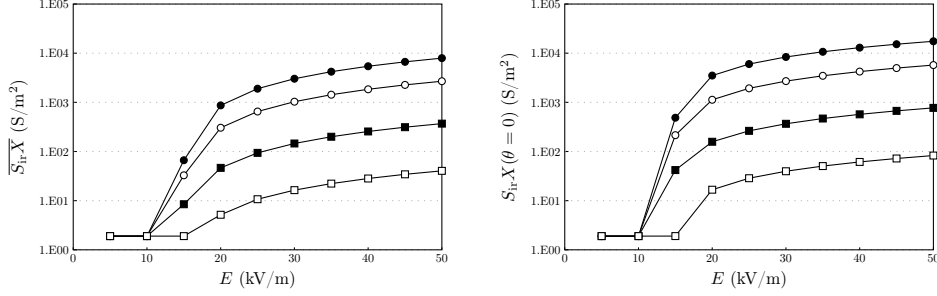


Figure 4: Membrane conductivity S_m computed by solving the static equation when $\sigma_e = 1$ S/m (\bullet), $\sigma_e = 0.1$ S/m (\circ), $\sigma_e = 0.01$ S/m (\blacksquare), $\sigma_e = 0.001$ S/m (\square).

Table 1: Parameters set to fit to the results given by [14, 3].

Variable	Symbol	Value	Unit
<i>Biological parameters</i>			
Extracellular conductivity	σ_e	5	S/m
Intracellular conductivity	σ_c	0.455	S/m
Capacitance	C_m	9.5×10^{-3}	F/m ²
Membrane surfacic conductivity	S_L	1.9	S/m ²
Cell radius	r	50	μm
Membrane thickness	δ	5	nm
<i>Model specific parameters</i>			
EP threshold	V_{rev}	1,5	V
EP switch speed	k_{ep}	40	V ⁻¹
EP characteristic time	τ_{ep}	1×10^{-6}	s ⁻¹
Reseal time	τ_{res}	1×10^{-3}	s ⁻¹
EP'd membrane surfacic conductivity	S_{ir}	2.5×10^8	S/m ²
<i>Numerical parameters</i>			
Simulation box size		200	μm
Grid points (side)	N	50	
Time pace	Δt	20	ns
Pulse duration	T_f	150	μs

Fig. 5 shows the numerical results using the parameters of Table 1. In order to visualize the membrane electropermeabilization we depict it with colored boxes and size by the value of the EP coefficient X . Note this is a visualization artefact since in the model membrane has no thickness.

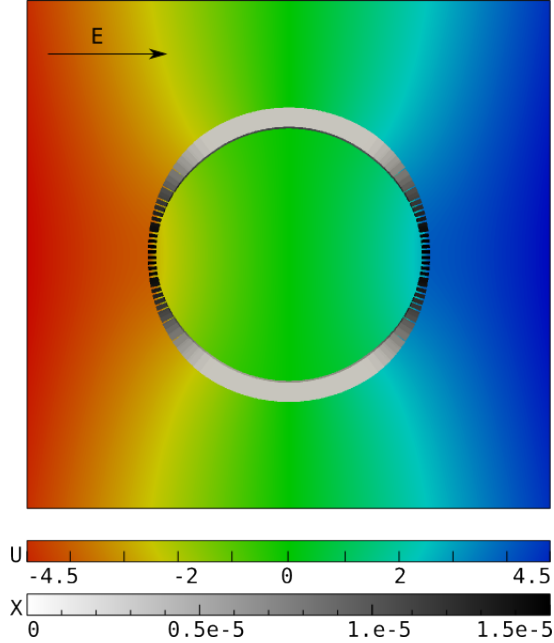


Figure 5: Results of simulations using the parameters of Table 1.

4.4.2 Main parameters influence

The key parameters of the model define the electropermeabilization coefficient \tilde{S}_m , that is k_{ep} , V_{rev} , S_{ir} and the characteristic times τ_{ep} and τ_{res} . A sensitivity analysis was lead to determine how solution to the model reacts to a variation of a specific parameter, as shown on Fig. 6. All the parameters defining the β function have a very small influence on the mean \bar{X} of X over the cell membrane. Even with for small values of k_{ep} the values of \bar{X} are only modified by a factor 2 (Fig. 6(a)). On the other hand, the fully porated membrane conductivity S_{ir} , which was first taken as $\sigma_c + \sigma_e/(2\delta)$, affects greatly the order of X (Fig. 6(c)).

4.4.3 Comparison with Neu and Krassowka models

The main difference between Neu and Krassowska models stands in the addition of an electroporation current $I_{ep} = N_{ep}i_{ep}$, instead of a direct description of the variations of the conductivity \tilde{S}_m .

The equation satisfied by the transmembrane potential in the model of Neu, Krassowska *et al.* [3] writes

$$-\sigma_c \partial_n U_c = C_m \partial_t [U] + S_L [U] + N_{ep} i_{ep} \quad (37)$$

where the ionic reversal currents have been neglected. N_{ep} is the pore density, obeying the

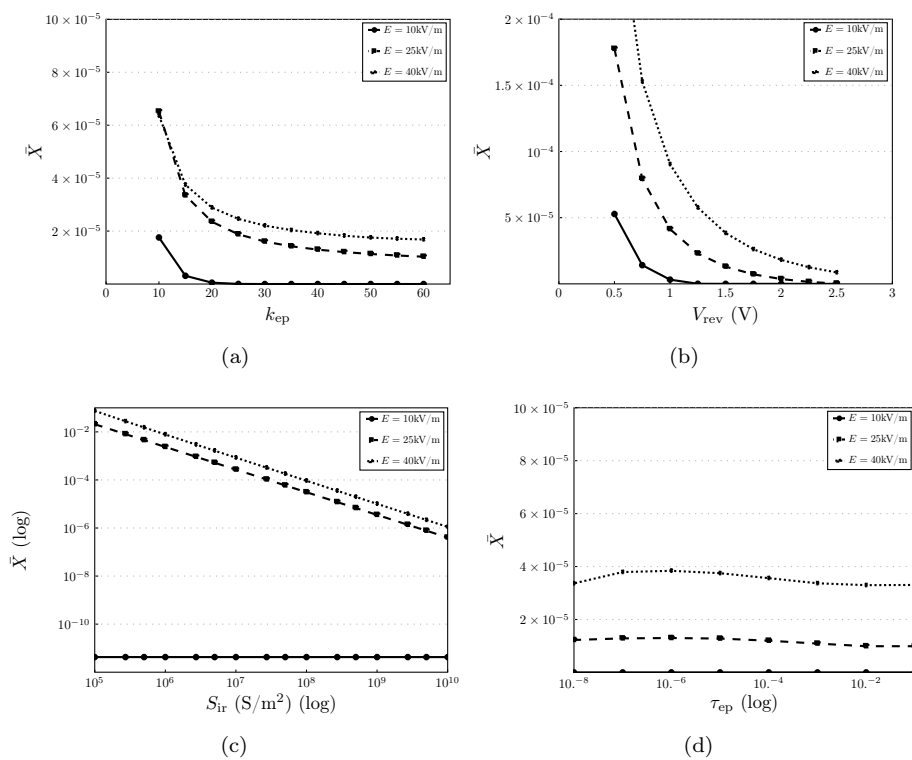


Figure 6: Variations of \bar{X} at 100 μs after the pulse delivery. Three magnitudes of electric pulse are considered: 10, 25 and 40 kV/m. A single parameter from table 1 is modified in each plot. Fig. 6(a) EP switch coefficient k_{ep} , Fig. 6(b) EP threshold voltage V_{rev} , Fig. 6(c) EP'd membrane surfacic conductivity S_{ir} , Fig. 6(d) EP speed τ_{ep} .

ordinary differential equation (parameters are emphasized with bold font):

$$\frac{dN_{\text{ep}}}{dt} = \alpha e^{([U]/V_{\text{rev}})} \left(1 - \frac{N_{\text{ep}}}{N_0} e^{-q([U]/V_{\text{rev}})^2} \right) \quad (38)$$

and i_{ep} is the current flowing through a single pore:

$$i_{\text{ep}}(v_m) = \frac{\pi r_m^2 \sigma RT}{F \delta} \frac{v_m (e^{v_m} - 1)}{\frac{w_0 e^{w_0 - n v_m} - n v_m e^{v_m}}{w_0 - n v_m} - \frac{w_0 e^{w_0 + n v_m} + n v_m}{w_0 + n v_m}} \quad (39)$$

with $v_m = [U] \times F/RT$ the adimensionalized TMP. Our model reproduces qualitatively the TMP behaviour in time and along the cell membrane, as shown in Fig. 7. In Fig. 8 we show that the conductivity variation in our model reproduces the electroperoration current $N_{\text{ep}} i_{\text{ep}}$.

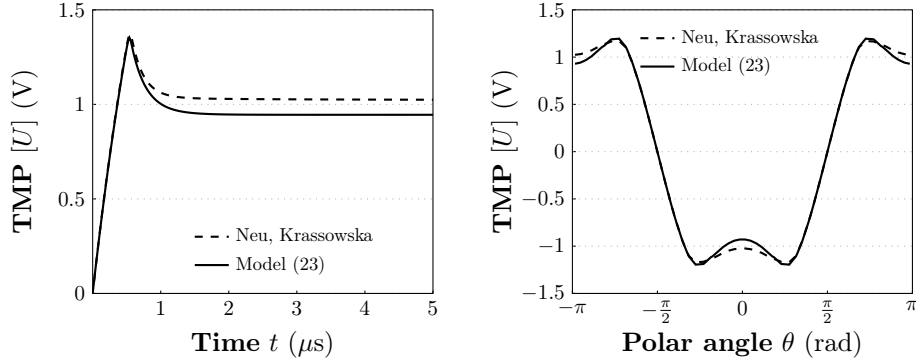


Figure 7: Comparison of the TMP obtained respectively with our model (solid lines) and with the model of Neu, Krassowska *et al.* (dashed), with parameters from table 1. Left : evolution of the TMP's at the cell pole. Right : values of the TMP's after $100\mu\text{s}$ along the perimeter of the circular cell.

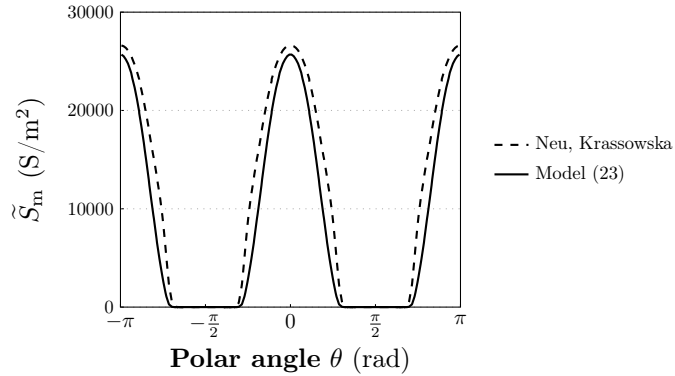


Figure 8: Comparison between the electroperoration current $N_{\text{ep}} i_{\text{ep}}$ of the model of Neu and Krassowska (dashed) and the membrane conductivity \tilde{S}_m of our model along the cell perimeter (solid).

4.4.4 Static vs dynamical model

In this paragraph we compare the long-time behaviour of the solution U_{dyn} to the dynamic model for a constant pulse with the solution U_{stat} to the static model.

Simulations is run to reach the time scale of the resealing speed τ_{res} (Fig. 9(a)). A constant pulse g is applied until the steady state of the dynamical system is reached. Comparisons are made between the obtained potentials U_{dyn} and U_{stat} with the error defined in (35). In Fig. 9(b) the continuous line shows that both potentials are close since the relative error is about 10^{-5} , however there is no convergence as the grid spacing h decrease. Actually the static model is not the exact steady-state of the dynamical model, due to the dynamics of X . It is possible to modify the dynamic model by replacing X by the function β , meaning that we omit the dynamics of the electropermeabilization:

$$\tilde{S}_m = S_L + \beta([U])(S_{\text{ir}} - S_L).$$

For this new model the solution to the dynamical model converges for long time to the static solution, due to the monotonicity of the function β . We let the reader verify this property.

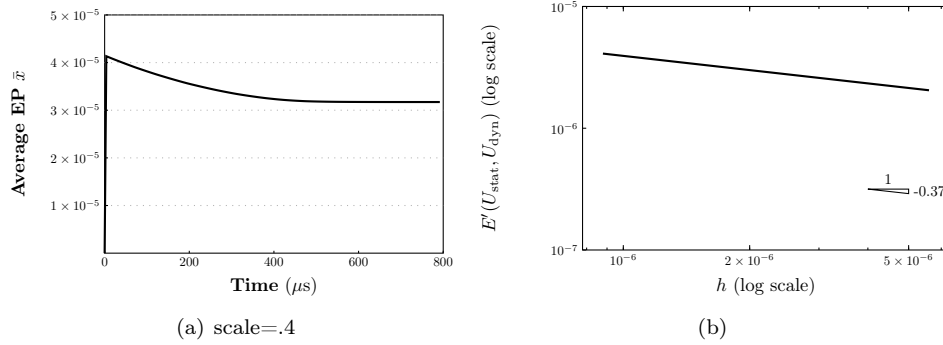


Figure 9: 9(a) : Electropermeabilization coefficient X during long time simulations. Steady state is reached after several hundreds of microseconds, which is larger than usual pulse duration. 9(b) : Convergence error between the steady state of U_{dyn} and the static potential U_{stat} , where in the dynamic model \tilde{S}_m is replaced by $S_L + \beta([U])(S_{\text{ir}} - S_L)$.

5 Conclusion

In this paper we have introduced two models of electropermeabilization. We first studied the static model, which is inspired by Ivorra *et al.*, showing existence and uniqueness result. We then derived a new dynamic model of cell electropermeabilization, which takes the permeabilizing time of the membrane into account. We studied mathematical properties of this new model. We then provided a second order finite differences method on cartesian grid to compute these models, and we eventually presented numerical simulations for both static and dynamic models, that corroborate the results of the most achieved model of Neu, Krassowska *et al.*

The main features of our models lie the fact that without loss of accuracy it is composed by a small number of parameters (mainly 4 parameters: S_{ir} , V_{rev} , and τ_{ep} , and τ_{res} for the dynamical system) compared with the sophisticated models with a tens of non measurable parameters of Neu, Krassowska *et al.* Therefore a forthcoming fitting of our models with the experimental data seems feasible, which is hardly the case for models with a large number of parameters.

From the biological point of view we highlight the fact that the static model can be used for very long pulses (around 1ms), but for short pulses around $10\mu\text{s}$ and below dynamics of the phenomenon have to be considered.

Acknowledgements

This research has been partly granted by the French national agency throughout the research projects INTCELL (2010-BLAN-916-04) and MEMOVE (2011-BS01-006-01).

References

- [1] F.M. André and J. Gehl *et al.* Efficiency of high - and low - voltage pulse combinations for gene electrotransfert in muscle, liver tumor and skin. *Human Gene Therapy*, 19, 2008.
- [2] M. Cisternino and L. Weynans. A parallel second order method for elliptic interface problems, accepted in *cicp*, 2012.
- [3] K. DeBruin and W. Krassowska. Modelling electroporation in a single cell. I. Effects of field strength and rest potential. *Biophysical Journal*, 77:1213–1224, Sept 1999.
- [4] K. DeBruin and W. Krassowska. Modelling electroporation in a single cell. II. Effects of ionic concentrations. *Biophysical Journal*, 77:1225–1233, Sept 1999.
- [5] D.E. Goldman. Potential, impedance and rectification in membranes. *J. General Physiology*, 27:37–60, 1943.
- [6] T. R. Gowrishankar, A. T. Esser, Z. Vasilkoski, K. C. Smith, and J. C. Weaver. Microdosimetry for conventional and supra-electroporation in cells with organelles. *Biochem Biophys Res Commun*, 341(4):1266–1276, Mar 2006.
- [7] A.L Hodgkin and B. Katz. The effect of sodium ions on the electrical activity of the giant squid axon. *J. Physiology*, 108:37–77, 1949.
- [8] L. Hodgkin and P. Horowicz. The influence of potassium and chloride ions on the membrane potential of single muscle fibres. *J. Physiol.*, 148:127–160, 1959.
- [9] L. Hodgkin and A. Huxley. A quantitative description of membrane current and its application to conduction and excitation in nerve. *J. Physiol.*, 117:500–544, 1952.
- [10] A. Ivorra, J. Villedemane, and L.M. Mir. Electrical modeling of the influence of medium conductivity on electroporation. *Physical Chemistry Chemical Physics*, 12(34):10055–10064, 2010.
- [11] M. Marty, G. Sersa, and J.-R. Garbay *et al.* Electrochemotherapy – an easy, highly effective and safe treatment of cutaneous and subcutaneous metastases: Results of esope (european standard operating procedures of electrochemotherapy) study. *E.J.C Supplements*, 4:3–13, 2006.
- [12] L.M. Mir. Therapeutic perspectives of *in vivo* cell electropermeabilization. *Bioelectrochemistry*, 53:1–10, 2001.

-
- [13] L.M. Mir. Electroporation of cells in tissues. Methods for detecting cell electropermeabilisation *in vivo*. In *Electroporation based Technologies and Treatment: proceedings of the international scientific workshop and postgraduate course*, pages 32–35, 14-20 November 2005. Ljubljana, SLOVENIA.
- [14] J. Neu and W. Krassowska. Asymptotic model of electroporation. *Physical Review E*, 53(3):3471–3482, Mar 1999.
- [15] J. Neu and W. Krassowska. Singular perturbation analysis of the pore creation transient. *Physical Review E*, 74(031917):1–9, Sep 2006.
- [16] S. Osher and J. A. Sethian. Fronts propagating with curvature-dependent speed: Algorithms based on hamilton-jacobi formulations. *J. Comput. Phys.*, 79(12), 1988.
- [17] M. Pavlin, T. Kotnik, D. Miklavcic, P. Kramar, and A.M. Lebar. Electroporation of planar lipid bilayers and membranes. *Advanced in Planar Lipid Bilayers and Liposomes*, 6(7), 2008.
- [18] R. Perrussel and C. Poignard. Asymptotic expansion of steady-state potential in a high contrast medium with a thin resistive layer. INRIA research report RR-7163. <http://hal.inria.fr/inria-00442659/fr/>, 2011.
- [19] G. Pucihar, T. Kotnik, B. Valič, and D. Miklavčič. Numerical determination of transmembrane voltage induced on irregularly shaped cells. *Ann Biomed Eng*, 34(4):642–652, Apr 2006.
- [20] G. Serša. Application of electroporation in electrochemotherapy of tumors. In *Electroporation based Technologies and Treatment: proceedings of the international scientific workshop and postgraduate course*, pages 42–45, 14-20 November 2005. Ljubljana, SLOVENIA.
- [21] J. Smith, K. Neu and W. Krassowska. Model of creation and evolution of stable electropores for DNA delivery. *Biophys. J.*, 86:2813–2826, May 2004.
- [22] J. Teissié. *In Vitro* cell electropermeabilization. In *Electroporation based Technologies and Treatment: proceedings of the international scientific workshop and postgraduate course*, pages 29–31, 14-20 November 2005. Ljubljana, SLOVENIA.
- [23] J. Teissié, M. Golzio, and M.P. Rols. Mechanisms of cell membrane electropermeabilization: A minireview of our present (lack of?) knowledge. *Biochimica et Biophysica Acta*, 1724:270–280, 2005.



**RESEARCH CENTRE
BORDEAUX – SUD-OUEST**

351, Cours de la Libération
Bâtiment A 29
33405 Talence Cedex

Publisher
Inria
Domaine de Voluceau - Rocquencourt
BP 105 - 78153 Le Chesnay Cedex
inria.fr

ISSN 0249-6399